# Accepted Manuscript


Characterizing segregation in the Schelling-Voter model

Inés Caridi, J.P. Pinasco, N. Saintier, P. Schiaffino

PII: S0378-4371(17)30611-8
DOI: http://dx.doi.org/10.1016/j.physa.2017.05.092
Reference: PHYSA 18378

To appear in: *Physica A*

Received date : 30 November 2016
Revised date : 4 May 2017

Please cite this article as: I. Caridi, J.P. Pinasco, N. Saintier, P. Schiaffino, Characterizing segregation in the Schelling-Voter model, *Physica A* (2017), http://dx.doi.org/10.1016/j.physa.2017.05.092

This is a PDF file of an unedited manuscript that has been accepted for publication. As a service to our customers we are providing this early version of the manuscript. The manuscript will undergo copyediting, typesetting, and review of the resulting proof before it is published in its final form. Please note that during the production process errors may be discovered which could affect the content, and all legal disclaimers that apply to the journal pertain.

ACCEPTED MANUSCRIPT

**Highlights**

- A mix of the classical Schelling segregation model with the Voter model is studied.
- In this mixed model an unhappy agent can change her place or her state to be happy.
- The main parameters are the propensity to change type and the density of empty spaces.
- Several segregation/extinction patterns appear in the parameter space.
- Different measures for the segregation patterns are studied.

ACCEPTED MANUSCRIPT

ACCEPTED MANUSCRIPT

*Manuscript
Click here to view linked References

# Characterizing Segregation in the Schelling-Voter Model

Inés Caridi[a,*], J.P. Pinasco[b], N. Saintier[b], P. Schiaffino[c]

[a]*Instituto de Cálculo UBA-CONICET,*
*Facultad de Ciencias Exactas y Naturales, Universidad de Buenos Aires,*
*Ciudad Universitaria, Pab. II, Int. Guiraldes 2160*
*(1428) Buenos Aires, Argentina.*
[b]*Departamento de Matemática and IMAS UBA-CONICET*
*Facultad de Ciencias Exactas y Naturales, Universidad de Buenos Aires,*
*Ciudad Universitaria, Pab I, Int. Guiraldes 2160,*
*(1428) Buenos Aires, Argentina.*
[c]*Departamento de Economía, Universidad Torcuato Di Tella,*
*Av. Figueroa Alcorta 7350, (1428) Buenos Aires, Argentina.*

## Abstract

In this work we analyze several aspects related with segregation patterns appearing in the Schelling-Voter model in which an unhappy agent can change her location or her state in order to live in a neighborhood where she is happy. Briefly, agents may be in two possible states, each one represents an individually-chosen feature, such as the language she speaks or the opinion she supports; and an individual is happy in a neighborhood if she has, at least, some proportion of agents of her own type, defined in terms of a fixed parameter $T$.

We study the model in a regular two dimensional lattice. The parameters of the model are $\rho$, the density of empty sites, and $p$, the probability of changing locations. The stationary states reached in a system of $N$ agents as a function of the model parameters entail the extinction of one of the states, the coexistence of both, segregated patterns with conglomerated clusters of agents of the same state, and a diluted region.

Using indicators as the energy and perimeter of the populations of agents in the same state, the inner radius of their locations (i.e., the side of the maximum square which could fit with empty spaces or agents of only one

*Corresponding author
*Email addresses:* ines@df.uba.ar (Inés Caridi), jpinasco@gmail.com (J.P. Pinasco), nsaintie@dm.uba.ar (N. Saintier), plschiaffino@gmail.com ( P. Schiaffino)

ACCEPTED MANUSCRIPT

type), and the Shannon Information of the empty sites, we measure the segregation phenomena. We have found that there is a region within the coexistence phase where both populations take advantage of space in an equitable way, which is sustained by the role of the empty sites.

*Keywords:* Schelling Model; Voter Model; Segregation; crowds

## 1. Introduction

In the last decades, international migration has been increasing ethnic diversity in different urban areas to date. Ethnic segregation in the way of ghettos might provide advantages for new migrants to the city, where they could find an established social network. Nevertheless, segregation can become problematic when it is associated with social exclusion and economic marginalization, even worse if inequalities persist across generations, limiting opportunities for health, employment and schooling, among other problems. Segregation is analyzed by different institutions across the world, see [1].

Residential segregation in terms of the concentration of ethnicity, nationality or socioeconomic level groups in different parts of a city has been one of the most important public socio-political topics all around the world for a long time. Before Schellings's works round the 1970s, it was commonly believed that residential segregation was caused by strong discriminatory preferences (racism, economic discrimination). Nevertheless, using an agent-based model, Schelling showed that mild discriminatory preferences and segregation patterns are compatible situations. He proposed a social model which captures mild and local individual preferences in terms of the choice of residence [2, 3, 4, 5, 6], assuming that in a population of two types of agents (races in the original work), every agent prefer to live surrounded by at least some proportion of agents of their own type. In his model, a set of agents are allowed to change their locations in order to satisfy their preferences. These individual choices can lead to segregation in the way of ghettos, clusters of agents of one predominant type of varied shapes and sizes. It is surprising that segregation occurs although no individual agent strictly seeks it, since individuals are tolerant to a mixed neighborhood. In this way, Schelling alerted that certain individual mechanisms can impact on segregated neighborhood patterns as an unintended consequence, and even modest levels of racial preferences can be amplified into high levels of global segregation.

In the classical descriptions of the model, two types of agents coexist on

ACCEPTED MANUSCRIPT

a square lattice with a proportion of empty sites. Every agent has a fixed tolerance level $T$, which is the threshold for the proportion of people of the opposite type she is willing to tolerate among her neighbors. When this threshold is reached, the agent becomes unhappy and decides to migrate to some empty site. Hence, agents have a utility function with two possible values (0 when she is happy and 1, when she is unhappy).

The Schelling model is based on the economic idea that an individual takes decisions according to a preference or a utility function, which depends on the local environment. Its results have drawn the economic community's attention because it is a clear example of the emergence of aggregate phenomena which are unseen by directly observing individual behaviors [7, 8, 9], and of a model of *critical-mass* phenomena, in which people's behavior depends on how many others are behaving in a specific way [10].

On the other hand, the fact that very simple rules for interacting agents lead to emergent properties such as segregation patterns, and their connection with a physical system such as the Ising model [11, 12], has made the Schelling model very interesting for the physicists' community [13, 14]. In the analogy with a physical system, agents are considered dummy particles, and the concept of utility function is replaced by the internal energy the particle stores. According to this interpretation, an increase in the happiness of the agent represents a decrease in her internal energy. Thus, an agent tries to minimize her energy (or maximizes her utility) by moving to another place.

There are different rules which govern the movement of agents: for example, moving only to empty spaces, or interchanging places, avoiding movements to closer or distant places. Many variants of the model include changes in the utility function, size of the neighborhood, and the availability of empty spaces to move in, among others, see for instance [15, 16, 17, 18, 19]. Recently, Vinkovic et al. [14] show that these movement rules matter to define the shape of the borders of the resulting clusters.

In a previous work [20], we wondered what could happen if an unhappy agent could change her position or change her own type in order to become happy. Although this does not make sense when we speak about racial characteristics, it does make sense in many social and economic situations, where an agent who is unhappy about her neighborhood can choose between trying to adapt to her neighbors or to migrate to a place which she deems better for her. Thus, we have mixed the Schelling and the Voter model, another well-known agent-based model introduced by Holley and Liggett [21], in which

ACCEPTED MANUSCRIPT

agents of two states (usually opinions) can change their states depending on those of their neighbors by following different types of interaction rules, see [22]. There, we have combined Schelling and Voter dynamics in the following way: at every step, an unhappy agent is selected at random, and she chooses to play one of two different games: either she migrates to another place where she will be happy (with probability $p$), or she changes her own type (with probability $1 - p$).

The Schelling-Voter model we have proposed is non-conservative in terms of the population type of agents (exchange is possible) but it is still conservative in terms of the whole population. In the variation of the Schelling model proposed by Gauvin et al. in [12], also the whole population is non-conservative. The authors consider an open city with a reservoir of agents of both populations outside the city and define a parameter of *welcome* to the city. They pay attention to the resulting vacancy density of the city, which is a non-fixed variable because of the possibility for external moves in both directions between the city and the reservoir. In particular, they analyse the shape of the borders conformed by the empty sites surrounding clusters of agents of the same population. In our model the number of empty spaces is fixed, although we vary it as one of the main parameters together with the propensity to change agent types. In particular, we study the role that the empty space plays either as borders of clusters or as available space inside clusters of agents of the same type.

In our previous work [20], we showed that the phase-diagram in the $(\rho, p)$ plane for a fixed tolerance $T$ can be roughly divided into four regions corresponding to qualitatively different kinds of final configurations: the extinction of one of the states, ghetto formation, coexistence of both states and diluted states. This last case involve sparse groups of agents (or isolated agents) over the grid with a lot of vacant sites. In the last three cases, both type of agents survive.

The aim of this paper is to further study the phase-diagram in a quantitative way by introducing some indicators:

1. The *perimeter* of the clusters of each population, an indicator which focuses on those agents who have lower values of utility because of their bordering location.
2. The *energy* of each population, defined in terms of links between neighbors, an indicator which takes into account a global utility function.
3. The *inner radius* of the clusters of each population, which gives the size

ACCEPTED MANUSCRIPT

of the maximum square which could fit without mixing populations.
4. The *Shannon's information* of the empty space, which gives information about the role that empty space is playing as a whole.

### *1.1. A Few words about the indicators*

Let us remark that the problem of pattern characterization is an interesting problem by itself, appearing in porous media, colloidal mixtures, percolation processes, statistical mechanics, probability theory, random and discrete geometry, image segmentation and classification, among many other fields of pure and applied sciences. We refer the interested reader to chapters 2 and 3 of [23], and the monograph [24] for some of these applications.

In the specific case of social sciences, the measure of residential segregation is a highly debated topic, and we refer only to [25] for a description and a history of the indicators, together with their main advantages and drawbacks, and the relevant bibliography. There are essentially five dimensions of segregation, and about 20 indicators were used to measure them.

In our work, two of these dimensions cannot be considered: *concentration* and *centrality*. The former refers to the density of the different groups and here each agent has always the same proportion of space, one site in the grid. The later studies the location of the groups respect to the center of the town, assuming that it has some additional value and it is exploited by one of the groups, however this is a dimension of the problem which is highly debated now due to decentralization and the growth of suburban residential neighborhoods. Let us recall that a Schelling model with this characteristic can be found in [17], see also [26].

The other three dimensions are *evenness*, *exposure* and *clustering*. This last dimension is the typical one studied for the classical Schelling model, where the agents only can change positions. The distribution, size, mean path, diameters, and number of final clusters of each population are the main indicators considered, both qualitatively (as in the original works of Schelling) and quantitatively (see for instance [11], and specially [18], where precise theoretical estimates were obtained about their size and distribution).

The *evenness* refers to the spatial distribution of the populations, and there are several possible ways to measure it. For example, each region of the grid is classified in terms of the proportion of individuals of each group, and a region is considered integrated whenever the values are close to the proportions in all the grid; let us observe that this is an entropy measure,

ACCEPTED MANUSCRIPT

and the Information Index was defined in this way by Theil. In this work we focus on the Shannon Information indicator for the empty spaces, in much the same spirit, in order to study the opportunities afforded to each population to change locations. This also has some relationship with the density of unwanted locations studied in [11]. Also, the inner radius is an evenness indicator, since it refers to a minimum volume controlled by each population.

Finally, the *exposure* refers to the mean number of connections that an agent has with the members of the other population, computed separately for each population. Although there are different measures, they depend basically on the number of links between agents of different populations. The more links an agent has, the higher is her exposure, and whenever the mean of the individual exposures of the members of one population is higher than the mean of the members of the other population, there exists a higher inequality between both groups.

This dimension is related to the energy, defined as a sum over the links in the grid, of a parameter $c$ which equals $-1$ for links between agents of the same population, $+1$ for links between agents of different populations, and 0 if one of the linked nodes is an empty space. A beautiful analysis of the relationship between economic utility, internal energy of a particle, and particle dynamics can be found in [14]. A key result in their analysis is that the deformation of the boundary of a cluster depends on the curvature, and the dynamics tries to flatten the surfaces. With a different argument, a similar result appears in the characterization of the equilibrium states given in [27], although not explicitly stated in this way.

In order to measure the *exposure*, we split the energy into two separate functions, each one summing only the links which contains at least one node among the one of the populations. We refer to them as the energy of the smallest and the biggest population. However, let us point out that they are not true energies, and they can increase or decrease after each step of the dynamics.

The role of the energy as a utility function, and its connection with the perimeter, was discussed in [27], where the authors prove that it is a Lyapunov function if only unhappy agents can interchange positions (observe that the dynamics in [27] is different, since there are no empty spaces, although the proofs can be easily adapted to our case).

These results in [14, 27] make the perimeter indicator worth studying: whenever clusters appear, the population with greater perimeter has an ex-

ACCEPTED MANUSCRIPT

panding concave frontier. When the dynamics stops, the empty spaces play a fundamental role: they form an insulating layer, reducing the contact between both populations; or they are located inside a cluster of one of the populations, and so they are available for only one of the groups. Here, the Shannon Information indicator helps to distinguish between both situations.

### *1.2. Motivation and related models*

In the last few years some related models have focused on the reconfiguration or coevolution of networks and agents (see for instance the review [28]). More precisely, agents located on some network interact with their neighbors and as a result, they change their type, or they break the link with one or more agents, pointing to new agents. These kind of models were motivated by different problems, like epidemics, evolutive game theory, political or ideological polarization and their interrelation with segregation.

For instance, in [29, 30], agents are located on a fully connected graph. The agent type is defined by her opinion about some issue, represented by $\pm 1$, and the dynamic process depends on two probabilities $p_1$ and $p_2$: given two selected agents, with probability $p_1$ they will agree on the same opinion, and with probability $1 - p_1$ they will redirect the link with probability $p_2$. The main question here is related to whether the graph disconnects as two disjoint components, each one sharing one of the opinions, or all the agents remain in a single component and only one opinion survives, see [31, 32]. Recently, a full mathematical proof of the existence of this transition was obtained in [33] for Erdos-Renyi graphs.

On the other hand, in [34, 35] an infectious process is suppressed depending on the rate of rewiring and the contagion rate. Let us also mention [36], where agents are located on a square grid, playing the Prisoner's Dilemma with their neighbors; here, the type of the agents is the strategy they play, namely cooperate or defect, and the number of neighbors of each type determines the payoff that some agent will obtain depending on their own type. Now, agents change their strategy depending on their own payoff and the payoff of one of their contacts, and whenever an agent persuades another agent to copy her strategy, a new neighbor is added. Here, this mechanism enables cooperators to survive, despite the strong motivation to become defectors.

The main difference with our model is that the network is fixed and agents cannot reconfigure it, so they must change locations to find more acceptable neighbors. Still, there are models where fixed networks are considered, and

ACCEPTED MANUSCRIPT

there also exists a coupling between some dynamic process and the influence of the neighbors.

In [37], the classical Schelling model was studied, and they considered a fraction of switching agents which can spontaneously change their type at some rate, regardless of the structure of their neighborhood as in our model. Let us mention that in their model there are no absorbent states, so there are interesting questions about metastability, time to reach these metastable states, and permanence.

Finally, in [38] the agents are located on a fixed regular lattice, and agents play one of the strategies cooperate or defect in the Prisoner's Dilemma game. Now, the probability to change from one strategy to the other is related both to the respective payoffs of the players, and the number of agents of each type in their neighborhood, reducing the chances to change if there are enough agents of the same type.

The paper is organized as follows: in Section §2 we will define precisely the model and we introduce the necessary notation. In Section §3 we will present the considered indicators, and in Sections §4 and §5 we will present the results and conclusions.

## 2. Schelling-Voter dynamics

From now on, we will use indistinctly "state" or "type" in reference to the agent variable which is allowed to change, although it may not necessarily represent the color or the race, but the language she speaks, or other social or anthropological variable such as a belief, an opinion, a strategy, or a custom.

We have performed simulations of the Schelling-Voter dynamics on a lattice of size $L \times L$ (using mainly $L = 50$) and free boundary conditions. By this, we understand a lattice of size $(L + 2) \times (L + 2)$ where the top and bottom rows, and the first and last columns are empty, so an agent located in the adjacent rows or columns will interact with few neighbors.

The neighborhood considered of each agent is the Moore neighborhood, which includes the eight cells which surround her.

At the beginning, a population of $N$ agents is placed at random on the lattice, and the state of each agent is selected at random with the same probability for both states; each agent is labeled as $b$ (black) or $r$ (red) in order to distinguish them. The density of empty sites is $\rho = 1 - \frac{N}{L^2}$.

ACCEPTED MANUSCRIPT

We introduce a critical tolerance $T$, the same for all agents, and we will say that an agent is unhappy whenever the ratio between the number of agents of the other state in her neighborhood and the total number of agents in her neighborhood is greater than $T$, otherwise we say that the agent is happy. Let us note that the actual possible values of $T$ are the discrete values of the form $a/c$ where $c$ takes any value from 1 to 8 and $a$, from 0 to $c$. We consider that an isolated agent is happy, not imposing a gregarious behavior.

Following the Schelling-Voter model introduced in [20], an additional parameter is needed. Let $p \in [0, 1]$ be fixed. Now, an unhappy agent can play either the Schelling dynamics with probability $p$, by trying to change her location by a new one selected at random among those locations where the agent will be happy, or the voter dynamics with probability $1 - p$, by trying to change her state. Probability $p$ can be interpreted as a balance between the ease and the difficulty for an agent to migrate and to adapt/learn/turn into a new state.

Let us recall that migration could not be possible if the agent is unhappy in any of the empty available spaces, so a moving agent will always improve her happiness, although she can generate new unhappy agents between both the old and new neighbors.

The change of type would depend on some probabilities $q_{b\to r}$ and $q_{r\to b}$, which can include both the number of agents of each state (globally measured), and the perceived prestige of each one of the populations (named $s \in (0, 1)$ for the prestige of state $b$, and $1 - s$ for the prestige of $r$), by following the attractiveness function of languages introduced in [39]:

$$q_{b\to r} = \frac{sN_r}{(N_b + N_r)} \qquad q_{r\to b} = \frac{(1-s)N_b}{(N_b + N_r)},$$

where $N_b$ (respectively, $N_r$) is the number of agents with state $b$ (resp., $r$). In order to preserve the symmetry, we have considered that the prestige of both states is the same value, $s = 1 - s = 1/2$.

## 3. Indicators of segregation patterns

A *configuration* of the system is defined by a vector $\mathcal{C} = \{c_1, c_2, ..., c_{L\times L}\}$ of size $L \times L$, where $c_i$ is the state of the $i$ site given by $c_i = 1$ if $i$ site is occupied by a $b$ agent, $c_i = -1$ if $i$ site is occupied by a $r$ agent and $c_i = 0$ if the $i$ site is empty. Each $i$ site has a fixed position on the lattice. Thus, $\mathcal{C}$ defines a pattern on the lattice.

ACCEPTED MANUSCRIPT

Recall that the initial configuration of $N$ agents is a random choice of $\mathcal{C}$ with the constraint that the value 0 is assigned to $L \times L - N$ sites (they will be the empty sites), and the values 1 or $-1$ for the remaining $N$ non-empty sites were assigned with the same probability. The final configuration of a realization is that achieved by the system when dynamics stop, or when very few changes have occurred for a fixed period of time.

As in the Schelling-Voter model it is possible the change of states, we are specially interested in the performance of each population at the final configuration. Due to symmetry considerations, it makes sense in the following, instead of speak about the *black* and *red* populations, to refer to the population which turns out to be the smallest one (*small* population) and the one which turns out to be the biggest one (*big* population).

For two values of the tolerance ($T = 0.18$ and $T = 0.30$ cases), examples of final configurations as a function of the vacancy density $\rho$ and the probability of changing the location $p$ are shown in Figures 1 and 2, being red the agents in the biggest population, and black the agents in the smallest one. Other values of tolerance up to $T = 0.5$ show similar qualitative results.

In order to characterize the resulting patterns and their boundaries, let us think about the network $g$ whose nodes are the sites on the lattice and whose links are the set of all the non-ordered pairs of neighboring sites. Thus, the set of nodes of $g$ has $n(g) = L \times L$ elements, and taking into account the boundary sites, which has a lower number of connections, the total number of links is $l(g) = (8(L^2 - 4L + 4) + 20(L - 2) + 12)/2$.

For a given configuration, the total number of $b$ and $r$ agents, $N_b$ and $N_r$, can be written as:

$$N_b = \frac{1}{2}\sum_{i=1}^{L\times L} c_i^2 + \frac{1}{2}\sum_{i=1}^{L\times L} c_i \qquad N_r = \frac{1}{2}\sum_{i=1}^{L\times L} c_i^2 - \frac{1}{2}\sum_{i=1}^{L\times L} c_i \tag{1}$$

where the index $i$ covers all the network sites, and $N = N_b + N_r$ is the number of agents or non-empty sites.

There are several magnitudes to measure segregation for the classical Schelling model, based on the size of the clusters [2, 40], cluster geometry [11], and number of unhappy agents whenever the system freezes due to the lack of available empty spaces to achieve comfortable neighborhoods. In the following subsections, we will define several indicators which measure different aspects of segregation patterns which take into account the rupture of symmetry due to changes of states, and they consider also the use of the

ACCEPTED MANUSCRIPT

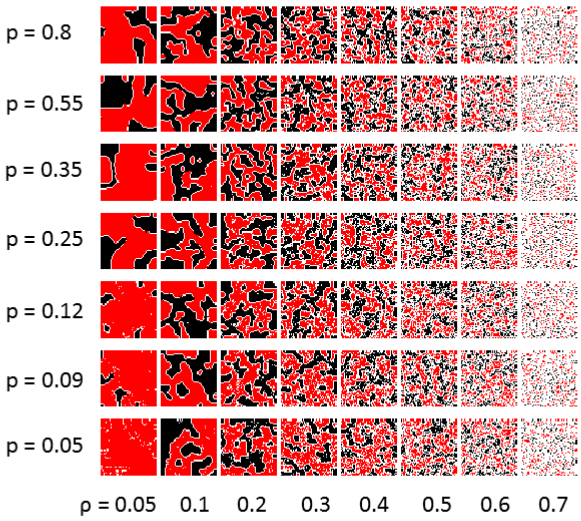


Figure 1: Examples of final configurations for different values of $\rho$ and $p$ for the value of tolerance $T = 0.18$ and $L = 50$. The smallest population is black and the biggest one is red. Plots in each column correspond to a fixed value of $\rho$ (following from the first column to the eighth, $\rho$ takes the values $0.05, 0.10, 0.20, 0.30, 0.40, 0.50, 0.60$ and $0.80$). Plots on each row correspond to a fixed value of $p$ (following from the lower up to the top, $p$ takes the values $0.05, 0.09, 0.12, 0.25, 0.35, 0.55$ and $0.80$).

ACCEPTED MANUSCRIPT

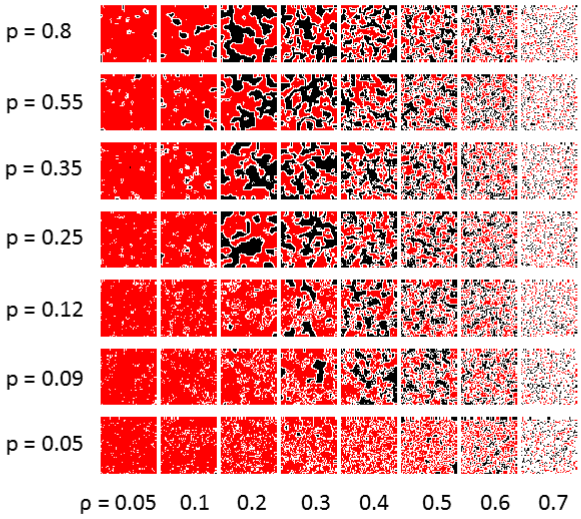


Figure 2: Examples of final configurations for different values of $\rho$ and $p$ for the value of tolerance $T = 0.30$ and $L = 50$. The smallest population is black and the biggest one is red. Plots in each column correspond to a fixed value of $\rho$ (following from the first column to the eighth, $\rho$ takes the values $0.05, 0.10, 0.20, 0.30, 0.40, 0.50, 0.60$ and $0.80$). Plots on each row correspond to a fixed value of $p$ (following from the lower up to the top, $p$ takes the values $0.05, 0.09, 0.12, 0.25, 0.35, 0.55$ and $0.80$.

ACCEPTED MANUSCRIPT

available space by the different populations.

*3.1. Perimeter indicator*

The local perimeter $p(i)$ of an agent occupying $i$ site is defined as the number of $i$'s neighboring sites that are either empty or occupied by an agent having the opposite state than the one of the agent at the site $i$:

$$p(i) = N_d + N_e$$

where $N_e$ is the total number of empty sites which are surrounding $i$ site (thus $c_j$=0 being $j$ a neighbour of $i$ on $g$) and $N_d$ is the total number of sites connected to $i$ site on $g$ which are occupied with agents in the opposite state that agent on site $i$ (thus $c_j \neq c_i$ and $c_j \neq 0$ with $j$ a neighbor of $i$ on $g$). Using Eq. 1, the local perimeter $p(i)$ can be rewritten as:

$$p(i) = 8 - \frac{1}{2} \sum_{k \in neig(i,g)} c_i^2 c_k^2 - \frac{1}{2} \sum_{k \in neig(i,g)} c_i c_k$$

where $neig(i, g)$ is the set of neighbors of $i$ site on the network $g$.

We have considered the perimeter of the big (respectively, small) population, called $P_{big}$ (resp., $P_{small}$), by applying the sum of $p(i)$ over all the $i$ sites occupied by one agent in the state of the big population (respectively small). $P_{big}$ and $P_{small}$ can be written as:

$$\begin{aligned} P_{big} &= \mathcal{L}_{empty-big} + \mathcal{L}_{big-small} \\ P_{small} &= \mathcal{L}_{empty-small} + \mathcal{L}_{big-small} \end{aligned} \tag{2}$$

where $\mathcal{L}_{empty-big}$ is the number of links on $g$ connecting an empty site with a site occupied by an agent in the state of the big population, $\mathcal{L}_{empty-small}$ is the number of pairs of $empty - small$ sites, and $\mathcal{L}_{big-small}$ is the total number of links on $g$ connecting two nodes occupied by agents in different states (one in state $b$ and the other one in state $r$). The indicators $P_{big}$ and $P_{small}$ capture information related with the frontiers of the populations, the boundaries of clusters, where the agents with lower chances of being happy are located.

In Figure 3 we illustrate the perimeter indicator for two extreme different final configurations. In the left panel, the small population makes up a ghetto surrounded by a boundary of empty sites, which limits both populations. The

ACCEPTED MANUSCRIPT

Figure 3: Example of two configurations of $5 \times 5$ sites. Left panel: the small population makes up a ghetto surrounded by empty sites which form a frontier with the big population, in this configuration $P_{big} = 4P_{small}$. Right panel: empty sites form a straight border which limits the big and small populations and contribute equally to both perimeters.

perimeter of the small population is smaller than that of the big population ($P_{big} = 4P_{small}$ in this particular case). This is caused by the convex shape of the ghetto, surrounded by empty sites, which results in more empty-big links than empty-small ones. The situation on the right panel gives rise to the same value of the perimeter for both populations, although the size of the populations are different. This is caused by the straight shape of the boundary of clusters.

Thus, the perimeter captures information related with the size and the shape of the frontiers among populations. This is the reason why we have decided not to normalize the perimeter value with respect to the size of the populations, in which case we would miss information regarding the borders, which is what we intend to record by considering this magnitude. In the following section, we apply a normalization related with the maximum possible value which the indicator can take on for $P$ to become independent of the system size.

### *3.2. Energy indicator*

This indicator is borrowed from [11]. An agent located at $i$ is happy if:

$$N_d - T(N_d + N_s) \leq 0, \tag{3}$$

being $N_s$ the total of agents on neighboring sites of $i$ on $g$ in the same type state than that occupying site $i$ (thus $c_j = c_i$ and $c_j \neq 0$). Hence, condition (3) can be rewritten as a property of the $i$ site:

$$-\sum_{j \in neig(i,g)} c_i c_j - (2T-1)c_i^2 \sum_{j \in neig(i,g)} c_j^2 \leq 0,$$

ACCEPTED MANUSCRIPT

in terms of the neighbors of the $i$ site on the network $g$.

By considering the sum over all the $(i, j)$ pairs of neighboring sites of each of the populations, we introduce the functions $E_{big}$ and $E_{small}$ which can be interpreted as the energy of the big and small subsystems respectively:

$$E_{big} = \sum_{<i,j>_{big}} c_i c_j - (2T-1) \sum_{<i,j>_{big}} c_i^2 c_j^2$$

$$E_{small} = \sum_{<i,j>_{small}} c_i c_j - (2T-1) \sum_{<i,j>_{small}} c_i^2 c_j^2$$

where the sums are over the $< i, j >_{big}$ pairs of neighboring big-big sites, and neighboring small-small sites.

Thus, we unfold the energy by separately considering the energy of each population as a subsystem, which can be rewritten in terms of the pairs of sites as:

$$\begin{aligned} E_{big} &= \mathcal{L}_{big-small} - T\mathcal{L}_{big-big} - T\mathcal{L}_{big-small} \\ E_{small} &= \mathcal{L}_{big-small} - T\mathcal{L}_{small-small} - T\mathcal{L}_{big-small} \end{aligned} \tag{4}$$

where $\mathcal{L}_{big-big}$ is the number of links connecting both nodes occupied by agents in the state of the big population and $\mathcal{L}_{small-small}$, the total links connecting both nodes occupied by agents in the state of the small population.

### *3.3. Inner radius indicator*

We define the inner radius for the big population, $nr_{big}$, as the side of the maximum square on the lattice for which all the sites inside are either occupied by agents of the big population or empty sites, and the analogous one for the inner radius of the small population, $nr_{small}$.

To simplify, the inner radius measures the maximum sublattice $nr \times nr$ inside a subpopulation. The empty sites inside that square could receive agents of the same population since they will be comfortable there, disregarding few empty sites in the boundary, since some of them are in contact with agents of the other population.

### *3.4. Shannon's information of empty sites*

Finally, the Shannon's information (or entropy) of an empty site $i$ takes into account only the amount of agents in the two possible states, and it is defined as

$$si(i) = -q_i \log(q_i) - (1 - q_i) \log(1 - q_i) \tag{5}$$

ACCEPTED MANUSCRIPT

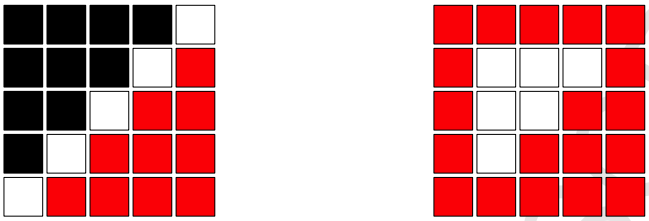

Figure 4: Example of two configurations of $5 \times 5$ sites. Left panel: empty sites form a straight border which limits both populations; in this case, each empty site contributes with the maximum value to Shannon's information, and $SI = 1$. Right panel: empty sites inside a cluster of agents of the same population; in this case, each empty site contributes with zero to Shannon's information, and $SI = 0$

where $q_i$ is the proportion of agents in the neighborhood of $i$ in the state $b$, and $1 - q_i$, the proportion in state $r$:

$$q_i = \frac{number\ of\ neighbors\ of\ i\ such\ that\ c_i = 1}{number\ of\ non\text{-}empty\ sites\ in\ i\text{'s}\ neighborhood},$$

we set $q_i = 0$ if all the neighbor sites of $i$ are empty, and we follow the usual convention that $x \log(x) = 0$ if $x = 0$.

The Shannon's information of the empty sites on the network $g$ is defined as the sum of the Shannon's information of each empty node $i$ normalized by the number of empty sites:

$$SI(g) = \frac{1}{N\rho} \sum_{i\ such\ that\ c_i=0} si(i) \tag{6}$$

The Shannon's information indicator of empty sites captures something we are interested in, which is the homogeneity of the neighborhoods of the empty sites. Figure 4 shows two different situations to illustrate $SI$. In the left panel the empty sites form a straight boundary separating two clusters of different types, and $si$ takes the maximum value 1 for each site (half of the occupied neighboring sites are $r$ and the other half, $b$). Therefore, $SI = 1$, reflecting a completely heterogeneous neighborhood for the empty sites. In the situation on the right panel, the empty sites are surrounded by other empty sites or occupied by agents of the same type. In this case, the contribution of each empty site to $SI$ is zero, which gives the result $SI = 0$, reflecting a completely homogeneous neighborhood for the empty sites.

ACCEPTED MANUSCRIPT

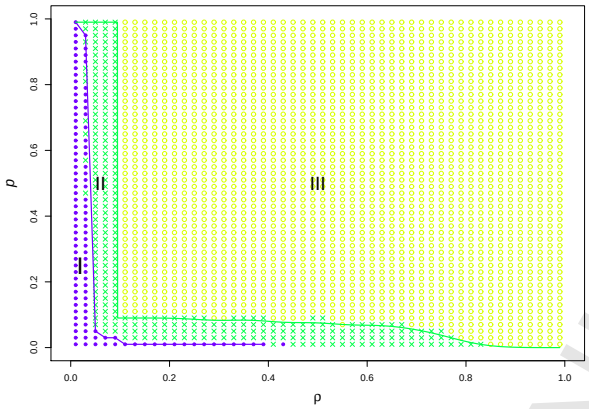


Figure 5: Phase diagram $\rho - p$ for tolerance $T = 0.30$ and $L = 50$. In region $I$ (dots, blue in the online version), the size of the minimum population is less than or equal to 10 per cent of $N$; in region $II$ (cross, green in the online version), it is between 10 and 45 per cent; in region $III$ (circles, yellow in the online version), the minimum population is greater than 45 per cent.

In the left panel of Figure 3, those empty sites which limit with one agent $r$ and three agents $b$, contribute with $si = 0.81$ each, and those with one agent $r$ and five agents $b$ (the corners of the border) contribute with $si = 0.65$ each. As a consequence, $SI = 0.73$.

According to this definition, a straight border of empty sites separating two clusters of different colors (vertical or horizontal for example) gives rise to a $si$ value near the maximum value 1 for each empty site because in this situation an empty site is surrounded by approximately half of the sites of one state and half of the other one. In the extreme case in which an empty site is surrounded by other empty sites or all agents of the same color, $si$ takes the minimum value 0. Thus, a set of empty sites inside a cluster does not contribute to the $SI$ magnitude.

## 4. Results

We have scanned the points of the phase diagram $\rho - p$ for tolerance $T = 0.30$. In the simulations, the agents evolve asynchronously. Results are obtained by averaging 100 realizations of 50000 time steps each, or until the systems stabilizes so that 99 per cent of the population is happy. Also, the curves in the figures below show the mean values over 100 realizations

ACCEPTED MANUSCRIPT

for each condition, and they are smoothed to avoid noise by averaging the results obtained in two following points of the parameters (as for example, taking two consecutive values of $\rho$).

Figure 5 shows three regions characterized by the size of the small population. In the first region $I$ (dots, blue in the online version), the size of the small population is less than or equal to 10% of $N$. In the second region $II$ (cross, green in the online version), it is between 10% and 45%. In the third region $III$ (circles, yellow in the online version), the minimum population is greater than 45% of the total population; we call its boundary the curve of coexistence, since the sizes of both populations are similar. However, as we will show below, some differences appear on the available empty spaces for each group, and the shapes of the clusters and their boundaries. Beyond $\rho = 0.6$, the system can be considered as a diluted one, there is too much empty space, so the system quickly reaches a final configuration that is almost identical to the initial one.

These regions were presented in our previous work [20], and can be mapped to extinction, ghetto formation, or coexistence. However, a sharper analysis of the coexistence region has motivated this work. In the following subsections, we present results for the previously defined indicators for the diagram $p - \rho$.

In order to obtain values of energy and perimeter not depending on the system size, we have normalized both magnitudes with respect to their maximum possible values:

- The maximum perimeter value for an agent is reached when all her neighbors are either empty sites or sites occupied by agents of the other state. In such case, the contribution to the perimeter is 8 and then the maximum perimeter is

  $$P_{max} = 16N_{eff},$$

  if we disregard the boundary conditions, being $N_{eff}$ the number of effective agents, which is $N_{eff} = N(1 - \rho)$.

- The maximum energy value for an agent is reached for $N_s = 8$ with $N_d = 0$, and therefore, the contribution to $E$ is $-8T$. Hence, by considering the whole system,

  $$E_{max} = 16TN_{eff}.$$

ACCEPTED MANUSCRIPT

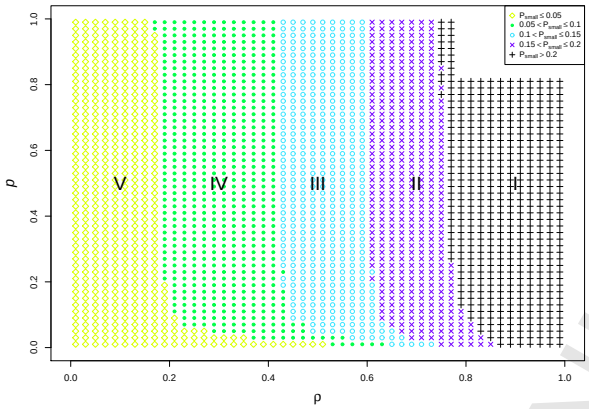


Figure 6: For each value of $p$ and $\rho$, symbols (colors in the online version) represent the normalized perimeter of the small population $P_{small}$: region $I$ (plus symbols, black in the online version) represent values greater than 0.2; region $II$ (cross, blue in the online version) represent values between 0.15 and 0.2; region $III$ (circles, skyblue in the online version) represent values between 0.1 and 0.15; region $IV$ (dots, green in the online version) represent values between 0.05 and 1; and region $V$ (circles, yellow in the online version) represent values less than 0.05.

### *4.1. Perimeter*

Figure 6 shows different regions according to the values of the normalized perimeter of the small population. We observe a clear pattern of values which increase depending on $\rho$ for any fixed value of $p$. The maximum values are found in the area of greater values of $\rho$ (region $I$), with values greater than 0.2. We have subdivided the $\rho - p$ diagram in regions where the normalized perimeter of the small population takes values between 0.15 and 0.2 ($II$), values between 0.1 and 0.15 ($III$), another one with values between 0.05 and 0.1 ($IV$), and finally by one whose perimeter of the minimum population is less than 0.05 ($V$). For small values of $p$ up to $p \approx 0.2$ we observe a shift of the boundaries of the regions to the right hand side, since in this region the coexistence phase occurs for higher values of $\rho$.

The corresponding image for the perimeter of the big population is showed in Figure 7; it shows a similar pattern from a value of $p \approx 0.2$, while the shape of the pattern is reversed up to this value.

For some fixed values of $\rho$ (0.05, 0.2 and 0.6) we have computed the mean value and the standard deviation of the normalized perimeter as a function of $p$, varying $p$ in the range from 0 to 1, see Figures 8 and 9. The plots show

ACCEPTED MANUSCRIPT

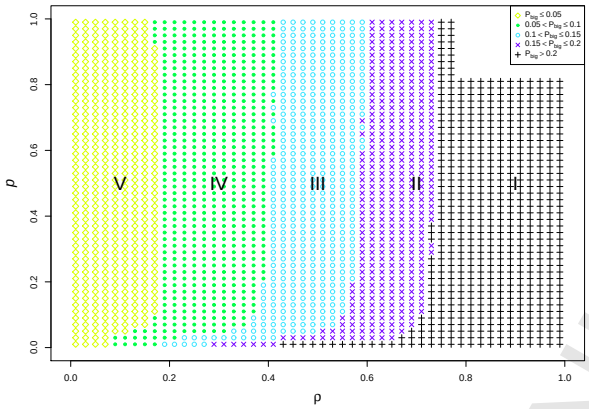


Figure 7: For each value of $p$ and $\rho$, symbols (colors in the online version) represent the normalized perimeter of the big population, $P_{big}$: region $I$ (plus symbols, black in the online version) represent values greater than 0.2; region $II$ (cross, blue) represent values between 0.15 and 0.2; region $III$ (circles, skyblue) represent values between 0.1 and 0.15; region $IV$ (dots, green) represent values between 0.05 and 1, and region $V$ (circles, yellow) represent values less than 0.05.

a value of $p$ for each $\rho$ in which the mean value of the perimeter indicators of the small and the big population coincide.

The standard deviation of the perimeters for the big and small populations overlap for $\rho = 0.2$ and $\rho = 0.6$, and let us note that $\rho = 0.05$ corresponds to extinction or ghetto formation in Figure 5. The maximum of the standard deviation is found near pairs $(\rho, p)$ where the transition from ghettos formation to coexistence occurs.

As a function of $\rho$ for a fixed $p$ value, the perimeter shows a very different behavior (see Figure 8). In the limit case of $\rho = 0$, the perimeter is null for both populations (there are no empty spaces, and only one population due to extinction of the other one), and after this value, the value for the two populations increases while the two curves become distinct (for the case of $p = 0.2$ and $p = 0.05$). Curves achieve different maximum values depending on $\rho$, and after their maximum they decrease until they are null again, when $\rho$ takes the value 1 (because, by definition, all the links belong to the *empty-empty* type).

In order to determine the region where the perimeters of the two popu-

ACCEPTED MANUSCRIPT

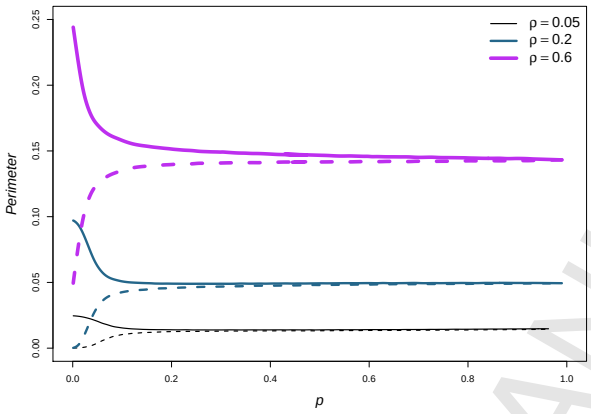


Figure 8: Normalized perimeter of the small population (dash line) and the big one (filled line) as a function of $p$ for different values of $\rho$ and $T = 0.3$.

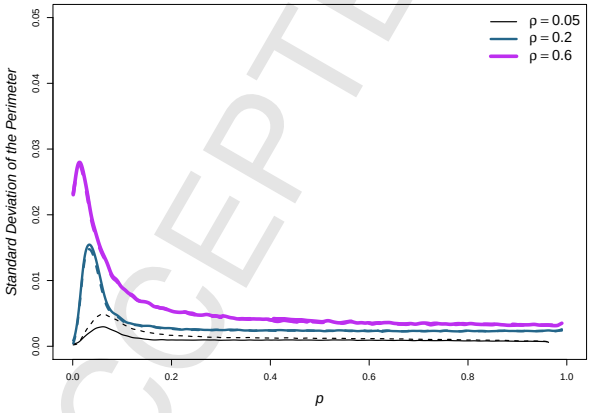


Figure 9: Standard deviation of the normalized perimeter of the small population (dash line) and the big one (filled line) as a function of $p$ for different values of $\rho$ and $T = 0.3$.

ACCEPTED MANUSCRIPT

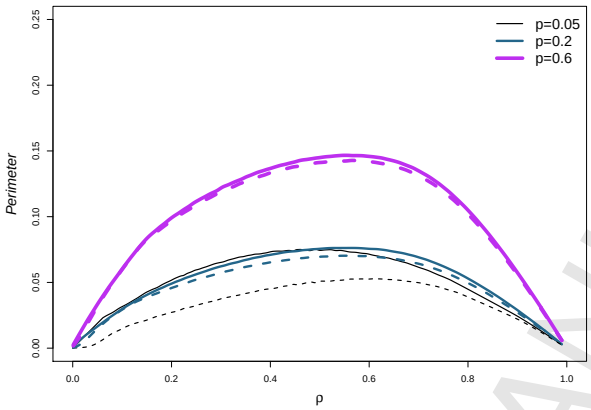


Figure 10: Normalized perimeter of the small population (dash line) and the big one (filled line) as a function of $\rho$ for different values of $p$ and $T = 0.3$.

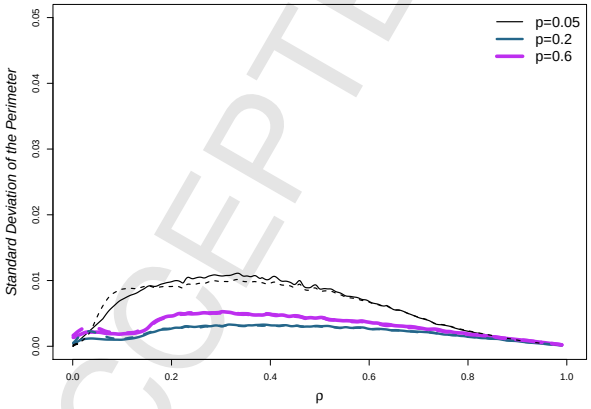


Figure 11: Standard deviation of the normalized perimeter of the small population (dash line) and the big one (filled line) as a function of $\rho$ for different values of $p$ and $T = 0.3$.

ACCEPTED MANUSCRIPT

lations are similar, we compute for each pair $(\rho, p)$ the magnitude

$$S_p = \frac{\bar{x} - \bar{y}}{\sqrt{\Delta x^2 + \Delta y^2}},$$

where $\bar{x}$ is the mean of the perimeter of the big population over all the 100 realizations, $\Delta x^2$ is the estimated variance of the perimeter of the big population, and $\bar{y}$ and $\Delta y^2$ are the analogous ones for the perimeter of the small population. The lower the value of $S_p$ is, the more comparable the values of the perimeters of both populations are. The magnitude $S_p$ is inspired on the statistics to test mean values among the perimeter of the two populations. Since the hypothesis of independence of the measures does not hold in this case, we do not use $S_p$ as a statistical test with an associated $p$-value. Thus, the purpose of applying $S_p$ to the perimeter indicator is to define different regions where the perimeters of the two populations are comparable to a greater or lesser extent.

Figure 12 shows regions with similar values of $S_p$. In region $I$ there are points for which $S_p$ takes values less than $-3$, and $II$ correspond to $-3 \leq S_p < -2$; in both the perimeter indicator are different. Region $III$ corresponds to values of $-2 \leq S_p < -1$, $IV$ to $-1 \leq S_p < -0.5$ and $V$ to $-0.5 \leq S_p$. We can consider that in regions $IV$ and $V$ the perimeter indicators are similar. Let us note that for very small values of $\rho$ or $p$, the perimeter indicators are far from similar, since one of the populations undergoes extinction or it is very close to it.

When the perimeters of both populations coincide, the number of links between an agent that belongs to the big population and an empty site (called *big-empty links* for simplicity) is approximately the same that the number of links between an agent that belongs to the small population and an empty site (called *small-empty links*), see Eq. (2). This can occur either because the empty sites play the role of borders of clusters of agents of different color or because no population takes advantage of the empty sites, a situation which could occur if both has roughly accumulated a set of empty sites inside their clusters, and not only one of them store empty sites.

### *4.2. Energy*

Normalized values of energy of small and big populations are shown in Figures 13 and 14 respectively. For the small population we define the region $I$ where $E < -0.35$, then in $II$ $-0.35 \leq E < -0.30$, in $III$ we have $-0.30 \leq$

ACCEPTED MANUSCRIPT

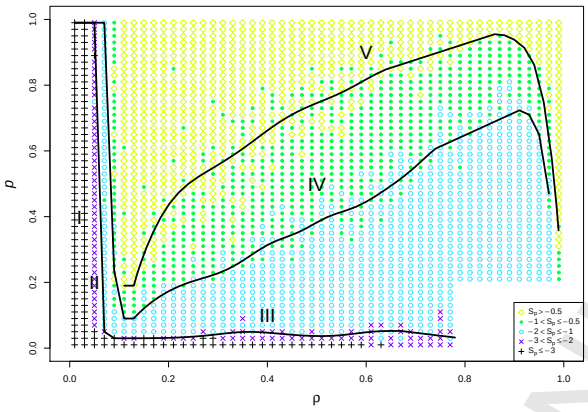


Figure 12: For each value of $p$ and $\rho$, symbols (colors in the online version) represent values of $S_p$ to compare the normalized perimeter of the both populations. Region $I$ (plus symbols, black in the online version) are those points for which $S_p$ takes values less than $-3$; region $II$ (cross, blue in the online version) are those points for which $-3 < S_p < -2$, in these cases we can consider both perimeters are not comparable; region $III$ (circles, skyblue in the online version) correspond to values of $-2 < S_p < -1$; region $IV$ (dots, green in the online version) correspond to values of $-1 < S_p < -0.5$ and region $V$ (circles, yellow in the online version) correspond to values of $-0.5 < S_p$.

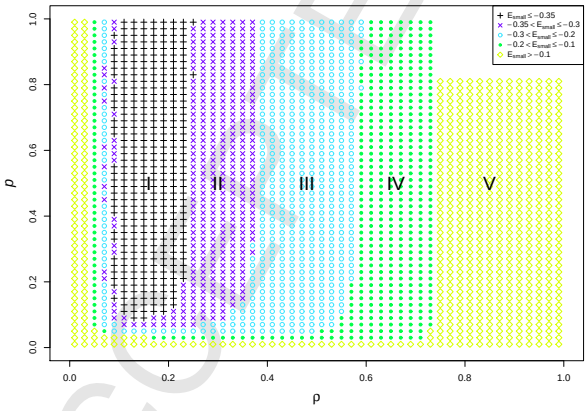


Figure 13: For each value of $p$ and $\rho$, symbols (colors in the online version) represent the normalized energy of the small population $E_{small}$: region $I$ (plus symbols, black in the online version) for values less than $-0.35$, $II$ (cross, blue) for values between $-0.35$ and $-0.3$; $III$ (circles, skyblue) for values between $-0.3$ and $-0.2$, $IV$ (dots, green) for values between $-0.2$ and $-0.1$ and $V$ (circles, yellow) for values greater than $-0.1$.

ACCEPTED MANUSCRIPT

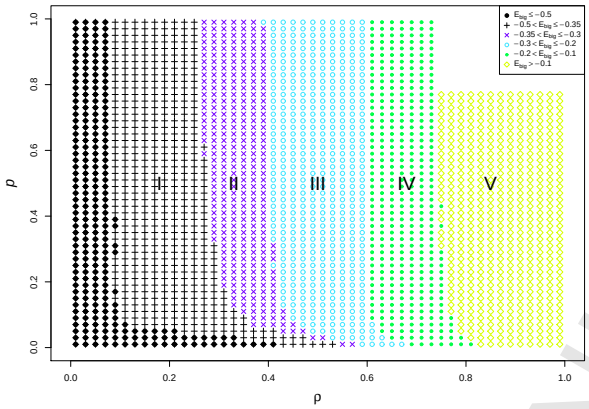


Figure 14: For each value of $p$ and $\rho$, symbols (colors in the online version) represent the normalized energy of the big population $E_{big}$: filled circles (black in the online version) for values less than $-0.5$; region $I$ (plus symbols, black in the online version) for values between $-0.5$ and $-0.35$; region $II$ (cross, blue in the online version) for values between $-0.35$ and $-0.3$; region $III$ (circles, skyblue) for values between $-0.3$ and $-0.2$, region $IV$ (dots, green in the online version) for values between $-0.2$ and $-0.1$ and region $V$ (circles, yellow in the online version) for values greater than $-0.1$.

$E < -0.20$, in $IV$ we have $-0.20 \leq E < -0.10$ and finally $E > 0.10$ in region $V$. Similar regions are defined for the big population.

We observe that both energies present a similar dependence on $\rho$ for any fixed value of $p$, except at low density regions, where one of the populations faces extinction, and also $E$ is almost constant for any fixed value of $\rho$, except for small $p$.

We compare the energy of the both populations as in the case of the perimeter indicator, by computing the magnitude $S_e$ defined as

$$S_e = \frac{\bar{x} - \bar{y}}{\sqrt{\Delta x^2 + \Delta y^2}}.$$

Now, $\bar{x}$ is the mean of the energy of the big population, $\Delta x^2$ is the estimated variance of the energy of the big population from the data, and $\bar{y}$ and $\Delta y^2$ are the analogous ones for mean and variance of the energy of the small population, see Figure 15.

We have used the same criterium that for the perimeter. However, the values of $S_e$ are mostly positives and thus, region $I$ correspond to values of

ACCEPTED MANUSCRIPT

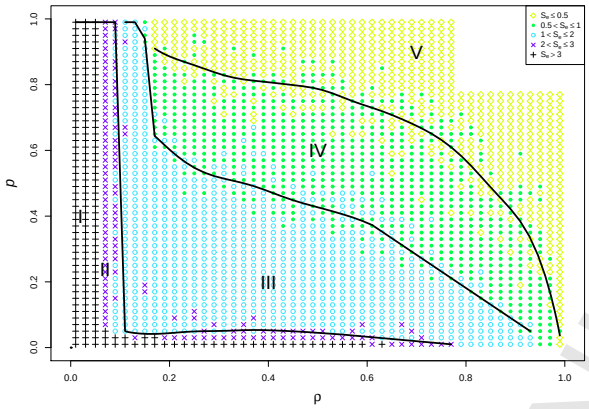


Figure 15: For each value of $p$ and $\rho$, symbols (colors in the online version) represent values of $S_e$ to compare the energy of the both populations. Region $I$ (plus symbols, black in the online version) are those points for which $S_e$ takes values greater than 3; region $II$ (cross, blue in the online version) correspond to values of $2 \leq S_e < 3$; region $III$ (circles, skyblue in the online version) correspond to values of $1 \leq S_e < 2$; region $IV$ (dots, green in the online version) correspond to values of $0.5 \leq S_e < 1$ and region $V$ (circles, yellow in the online version) correspond to values of $S_e < 0.5$.

$S_e$ greater than 3, in region $II$ we have $2 \leq S_e < 3$, in $III$ $1 \leq S_e < 2$, in $IV$ $0.5 \leq S_e < 1$ and in region $V$ we have $S_e < 0.5$.

Then, in the regions where the values of the energy are similar (regions $I$ and $II$) we have $\mathcal{L}_{big-big} \approx \mathcal{L}_{small-small}$, see Eq. (4). Thus, the composition of clusters of both populations are similar.

Let us observe that, as connections between agents and empty sites are not considered in the definition of the energy, this indicator gives no information about empty sites inside the clusters of each population.

### *4.3. Inner radius*

Figure 16 shows values of inner radius for some values of $p$ as a function of $\rho$ and Figure 17 shows the inner radius for some values of $\rho$ as a function of $p$. From them, it is clear that for each value of $p$, beyond certain value of $\rho$, the inner radius of both populations overlap.

We have computed the magnitude $S_r$, similar as the ones defined for perimeter and energy indicators. Figure 18 shows regions for different limit values of $S_r$. In this case, the considered values of $S_r$ to obtain the level curves are less than the ones for $S_p$ and $S_e$.

ACCEPTED MANUSCRIPT

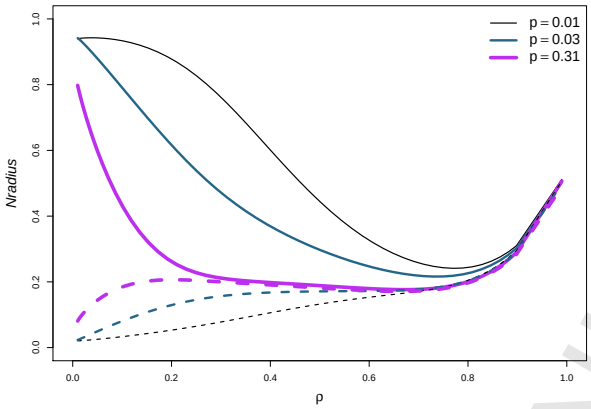


Figure 16: For some values of $p$, curves of inner radius of the small population, $nr_{small}$ (dash line) and that of the big one $nr_{big}$ (filled line) as a function of $\rho$ and $T = 0.3$.

Now, the main difference with the previous indicators is that the level curves of $S_r$ characterize the probability $p$, since they are almost parallel to the axis $\rho$ in this region (which corresponds with the coexistence region of the phase diagram in Figure 5).

### *4.4. Shannon information of empty sites*

Finally, we compute the Shannon Information for the empty sites for each final configuration of the phase diagram by considering the definition of $SI$ (i.e., not considering empty neighboring sites to compute probabilities). Figure 19 shows values of $SI$ as a function on $\rho$ and $p$. Region $I$ are those points for which $SI$ takes values less than 0.1, region $II$ corresponds to values of $0.1 \leq SI < 0.15$, region $III$ corresponds to values of $0.15 \leq SI < 0.20$, $IV$ to $0.2 \leq SI < 0.23$; and region $V$ corresponds to $0.23 \leq SI$.

A value $SI = 1$ means that all the empty sites are surrounded by half of the occupied sites in state $b$ and by other half by agents in the opposite state $r$, regardless of how many occupied sites there are in their neighborhood. If all the neighboring sites of an empty site are empty, the contribution to $SI$ is zero. The same will happen if all the occupied sites correspond to agents of the same color. Hence, $SI$ distinguishes homogeneous neighborhoods (greater values of $SI$) from heterogeneous ones (small values of $SI$). In the region of greater values of $SI$, empty sites are mainly playing the role of boundaries of clusters of different populations.

ACCEPTED MANUSCRIPT

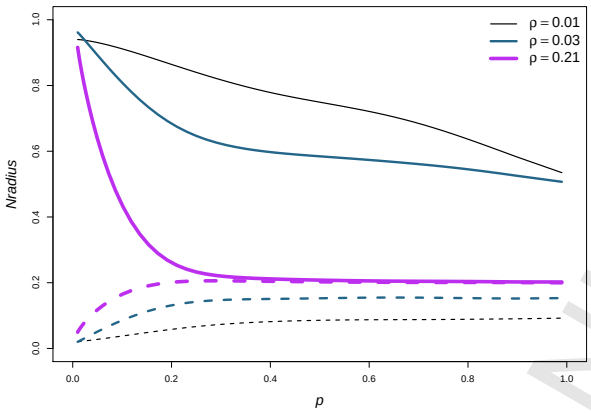


Figure 17: For some values of $\rho$,curves of inner radius of the small population, $nr_{small}$ (dash line) and that of the big one $nr_{big}$ (filled line) as a function $p$ and $T = 0.3$.

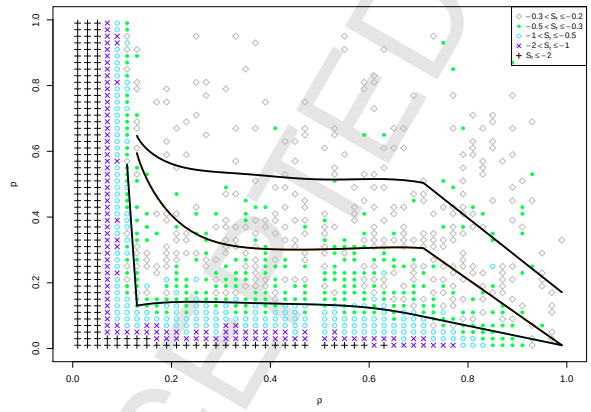


Figure 18: For each value of $p$ and $\rho$, symbols (colors in the online version) represent values of $S_r$ to compare the inner radius of the both populations. Region $I$ (plus symbols, black in the online version) are those points for which $S_r$ takes values less than $-2$; region $II$ (cross, blue in the online version) correspond to values of $-2 \leq S_r < -1$; region $III$ (circles, skyblue in the online version) correspond to values of $-1 \leq S_r < -0.5$; region $IV$ (dots, green in the online version) correspond to values of $-0.5 \leq S_r < -0.3$; region $V$ (circles, grey in the online version) correspond to values of $-0.3 \leq S < -0.2$.

ACCEPTED MANUSCRIPT

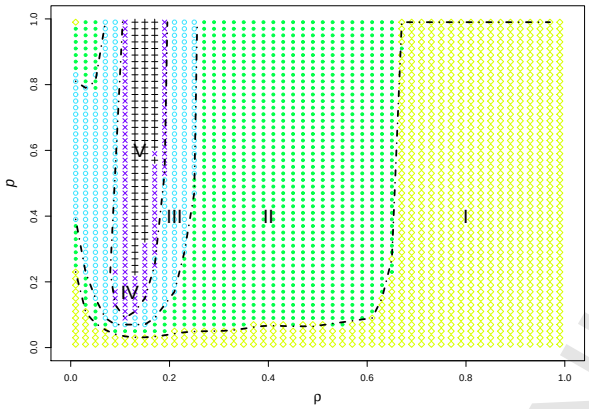


Figure 19: Shannon Information of the empty sites normalized by the total of empty sites as a function of $\rho$ and $p$. Region $I$ (circle symbols, yellow in the online version) are those points for which $SI$ takes values less than 0.1; region $II$ (dots, green in the online version) correspond to values of $0.1 \leq SI < 0.15$; region $III$ (circle, skyblue in the online version) correspond to values of $0.15 \leq SI < 0.20$; region $IV$ (cross, blue in the online version) correspond to values of $0.2 \leq SI$.

## 5. Conclusions

In this paper we have studied the behavior of a model which combines the Schelling and Voter dynamics. In this model, the unhappy agents can not only move elsewhere but also adapt to a new state in order to achieve a comfortable neighborhood.

Using some indicators of segregation, such as the energy, perimeter, inner radius of the big and small populations, and the Shannon information of the empty sites, we characterize some differences in the region of the coexistence, region $III$ in Figure 5.

Let us note that the intersection of regions $IV$ and $V$ in Figure 12 with regions $I$ and $II$ in Figure 15, gives rise a region where we can consider that the perimeter and the energy of both populations are similar, i.e., within this region the populations are similar in terms of the number of agents, the size of their frontiers (perimeter indicator), and the cluster structure (energy indicator). From Figure 2 we can observe that the final configurations in this region show winding curves as boundaries of the clusters, in the sense that neither of the populations is confined to ghettos, and the concavity of the boundary alternates. As we described in Section 2, ghettos show mainly

ACCEPTED MANUSCRIPT

convex borders surrounded by empty sites, and in this case, the population of the ghetto would have a smaller perimeter. The more different the perimeters of both populations are, it is possible to find empty sites that fall within one of the populations, the one which has greater values of the perimeter.

We can consider the difference of perimeters as an indicator of the different territorial control, and we could interpret this as the control over the available space by one population in order to occupy it in the future with agents of its own type, or to destine it to other uses, like a recreational space. The Shannon information of empty sites is maximized when the empty sites are surrounded evenly by agents of both populations.

On the other hand, populations with lower energy has more massive clusters. The presence of empty sites within one of the populations prevents that this population reaches even lower energy values. Again, both populations will have similar energy values whenever the composition of the clusters are similar.

So, in the intersection region referred above, both the number of agents and the mean number of connections between agents of the same type are similar, and no population takes any advantage of the empty spaces. Moreover, we can check from Figure 18 that the inner radius of both populations are almost equal in this region.

Hence, the region of the diagram in which the perimeters and energies of the two populations are similar reveals the set of parameters where the use of the space is almost the same for both populations. We conclude that in this region the population must not be overcrowded, a situation in which the mobility is restricted due to space constraints, nor too diluted, a situation in which there are no reasons to migrate nor to change state.

This last phenomena can be caused mainly by two very different reasons. First, both states are roughly equivalent. This is the case of similar status of languages, affording near equal economic or social opportunities for its speakers (i.e., English and French in Canada, or the different languages spoken in Spain). Several cases of coexistence of languages can be understood from this perspective. A second reason is the difficulty to change states: we can consider as a paradigmatic example languages which use different grammatical structures, phonology, phonetics, and even logographic versus alphabetic representations (as in the case of Indo-European and Asian languages). However, in order to reach an almost identical territorial distribution of the agents, we need a similar initial number of agents of each type, and we are not aware of real examples of this situation.

ACCEPTED MANUSCRIPT

There are several possible extensions of the model, let us mention the ones that we consider the most interesting. First, as Schelling pointed out, assigning different tolerances for both populations could generate important changes in the final configurations. Moreover, each agent may have her own tolerance parameter, and we can consider it as an opinion variable which evolves with time whenever agents interact. In this way, the model can reflect the changes that occur in the social mechanism itself. Also, the individual propensity to change locations or languages could be different for each agent. The influence of fashion or the public policies directed to preserve endangered languages can be modeled by varying these probabilities along the simulation. Let us stress that the model can be made more realistic by introducing survey data to define the tolerance, as Bruch and Mare did in [41], with data from Los Angeles, Boston and Detroit.

More heterogeneity could be added in other ways. We can think of a mix between the Schelling segregation model and the Axelrod model of dissemination of cultures, see [42]. We conjecture that in this case segregation will be reached quickly.

Finally, a game theoretic interpretation as in references [36, 38] suggests natural extensions of the model. Since the Middle Ages, students and scholars migrated to universities or institutions where their individual interests were better represented or recognized; today we observe this behavior also in football and basketball players, among other sports and activities. Briefly, we can consider the strategies of a player as her type, and her pay-off now depends on her location on the grid, possibly in a dynamical way. Now, she can migrate or change strategies to increase her pay-off. We expect very different patterns in this case.

## Acknowledgments

This research was partially supported by Grants 20020100100400 from University of Buenos Aires, and ANPCyT PICT2012 0153. IC, JPP and NS are members of CONICET, Argentina.

## References

[1] Migration Policy Institute, http://www.migrationpolicy.org (accessed 10.31.16).

ACCEPTED MANUSCRIPT

[2] T.C. Schelling, Models of segregation, American Economic Review 59 (1969) 488-493.

[3] T.C. Schelling, Dynamic models of segregation, Journal of Mathematical Sociology 1 (1971) 143-186.

[4] T.C. Schelling, On the ecology of micromotives, in The corporate society, Macmillan Education UK, 1974. 19-64.

[5] T. C. Schelling, A process of residential segregation: neighborhood tipping, in Racial Discrimination in Economic Life, A.H. Pascal (ed.), Lexington Books, Lexington, MA, 1972.

[6] T.C. Schelling, Micromotives and Macrobehavior, WW Norton & Co., New York, 1978.

[7] K. J. Arrow, What Has Economics to Say About Racial Discrimination?, Journal of Economic Perspectives 12 (1998) 91-100.

[8] W. A. V. Clark, Residential preferences and neighborhood racial segregation: a test of the Schelling segregation model, Demography 28 (1991) 1-19.

[9] Y. M. Ioannides, T. N. Seslen, Neighborhood wealth distributions, Economics Letters 76 (2002) 357-367.

[10] N. E. Aydinonat, The invisible Hand in Economics, How economists explain unintended social consequences, London, New York: Routledge, 2008.

[11] L. Gauvin, J. Vannimenus, J.P. Nadal, Phase diagram of a Schelling segregation model, The European Physical Journal B 70 (2009) 293-304.

[12] L. Gauvin, J.-P. Nadal, J. Vannimenus, Schelling segregation in an open city: a kinetically constrained Blume-Emery-Griffiths spin-1 system, Physical Review E 81 (2010) 066120.

[13] E. V. Albano, Interfacial roughening, segregation and dynamic behavior in a generalized Schelling model, Journal of Statistical Mechanics: Theory and Experiment 2012 (2012) P03013.

ACCEPTED MANUSCRIPT

[14] D. Vinkovic, A. Kirman, A physical analogue of the Schelling model, Proceedings of the National Academy of Sciences 103 (2006) 19261-19265.

[15] J. Zhang, A dynamic model of residential segregation, Journal of Mathematical Sociology 28 (2004) 147-170.

[16] L. DallAsta, C. Castellano, M. Marsili, Statistical physics of the Schelling model of segregation, Journal of Statistical Mechanics: Theory and Experiment, 2008 (2008) L07002.

[17] J. K. Shin, M. Fossett, Residential segregation by hill-climbing agents on the potential landscape, Advances in Complex Systems 11 (2008) 875-899.

[18] C. Brandt, N. Immorlica, G. Kamath, R. Kleinberg, An analysis of one-dimensional Schelling segregation, Proceedings of the forty-fourth annual ACM symposium on Theory of computing, ACM (2012) 789-804.

[19] K. A. Hawick, Multiple Species Phase Transitions in Agent-Based Simulations of the Schelling Segregation Model, Preprint, 2013.

[20] I. Caridi, F. Nemiña, J. P. Pinasco, P. Schiaffino, Schelling-voter model: an application to language competition, Chaos, Solitons & Fractals 56 (2013) 216-221.

[21] R. A. Holley, T. M. Liggett, Ergodic Theorems for Weakly Interacting Infinite Systems and the Voter Model, The Annals of Probability 3 (1975) 643-663.

[22] C. Castellano, F. Santo, V. Loreto, Statistical physics of dynamics, Reviews of Modern physics 81 (2009) 591-646.

[23] D. Stauffer, A. Aharony, Introduction to percolation theory, 2nd ed., CRC Press, 1994.

[24] P. Soille, Morphological image analysis: principles and applications, Springer-Verlag Berlin Heidelberg, 2004.

ACCEPTED MANUSCRIPT

[25] J. Iceland, D. H. Weinberg, E. Steinmetz, Racial and Ethnic Residential Segregation in the United States: 1980-2000, U. S. Census 2000 Special Reports. Bureau of Census 2002.

[26] L. Gauvin, A. Vignes, J.-P. Nadal, Modeling urban housing market dynamics: can the socio-spatial segregation preserve some social diversity?, Journal of Economic Dynamics and Control 37 (2013) 1300-1321.

[27] M. Pollicott, H. Weiss, The dynamics of Schelling-type segregation models and a nonlinear graph Laplacian variational problem, Advances in Applied Mathematics 27 (2001) 17-40.

[28] M. Perc, A. Szolnoki, Coevolutionary games - a mini review, BioSystems 99 (2010) 109-125.

[29] S. Gil, D. H. Zanette, Coevolution of agents and networks: Opinion spreading and community disconnection, Physics Letters A 356 (2006) 89-94.

[30] D. H. Zanette, S. Gil, Opinion spreading and agent segregation on evolving networks, Physica D: Nonlinear Phenomena 224 (2006) 156-165.

[31] F. Vázquez, V. M. Eguíluz, M. San Miguel, Generic absorbing transition in coevolution dynamics, Physical Review Letters 100 (2008) 108702.

[32] R. Durrett, J. P. Gleeson, A. L. Lloyd, P. J. Mucha, F. Shi, D. Sivakoff, J. E. S. Socolar, C. Varghese, Graph fission in an evolving voter model, Proceedings of the National Academy of Sciences, 109 (2012) 3682-3687.

[33] R. Basu, A. Sly, Evolving voter model on dense random graphs, Preprint 2015, arXiv:1501.03134.

[34] V. Marceau, P. A. Noël, L. Hébert-Dufresne, A. Allard, L. J. Dubé, Adaptive networks: Coevolution of disease and topology, Physical Review E 82 (2010) 036116.

[35] D. H. Zanette, S. Risau-Gusmán, Infection spreading in a population with evolving contacts, Journal of Biological Physics 34 (2008) 135-148.

[36] A. Szolnoki, M. Perc, Z. Danku, Making new connections towards cooperation in the prisoner's dilemma game, Europhysics Letters 84 (2008) 50007.

ACCEPTED MANUSCRIPT

[37] A. Hazan, J. Randon-Furling, A Schelling model with switching agents: decreasing segregation via random allocation and social mobility, The European Physical Journal B 86 (2013) 421.

[38] A. Szolnoki, Z. Wang, M. Perc, Wisdom of groups promotes cooperation in evolutionary social dilemmas, Scientific Reports 2, Article576 (2012).

[39] D. M. Abrams, S. H. Strogatz, Linguistics: Modelling the dynamics of language death, Nature 424 (2003) 900-900.

[40] R. Pancs, N. J. Vriend, Schelling's spatial proximity model of segregation revisited, Journal of Public Economics 91 (2007) 1-24.

[41] E. E. Bruch, R. D. Mare, Neighborhood Choice and Neighborhood Change 1, American Journal of sociology 112 (2006) 667-709.

[42] R. Axelrod, The dissemination of culture - A model with local convergence and global polarization, Journal of Conflict Resolution 41 (1997) 203-226.

ACCEPTED MANUSCRIPT